hearts

Article

Novel PITX2 Homeodomain-Contained Mutations from ATRIAL Fibrillation Patients Deteriorate Calcium Homeostasis

Adela Herraiz-Martínez [1,2,†], Carmen Tarifa [1,2,†], Estefanía Lozano-Velasco [3,†], Verónica Jiménez-Sábado [4], Sergi Casabella [1,2], Francisco Hernández-Torres [3], Houria Daimi [3], Eduardo Vázquez Ruiz de Castroviejo [5], Eva Delpón [6], Ricardo Caballero [6], Amelia Aránega [3], Diego Franco [3,‡] and Leif Hove-Madsen [1,2,5,*,‡]

1 Department of Experimental Pathology, Biomedical Research Institute Barcelona (IIBB-CSIC),
   08036 Barcelona, Spain; aherraiz@santpau.cat (A.H.-M.); carmen.tarifa@cnic.es (C.T.);
   scasabella@santpau.cat (S.C.)
2 Cardiac Rhythm and Contraction Group, Biomedical Research Institute IIB Sant Pau, 08025 Barcelona, Spain
3 Department of Experimental Biology, University of Jaén, 23071 Jaén, Spain; evelasco@ujaen.es (E.L.-V.);
   fraheto@ujaen.es (F.H.-T.); daimihouria@gmail.com (H.D.); aaranega@ujaen.es (A.A.); dfranco@ujaen.es (D.F.)
4 Centro de Investigación Biomédica En Red Cardiovascular (CIBERCV), 28029 Madrid, Spain;
   vjimenezs@santpau.cat
5 Cardiology Unit, Regional Hospital "Ciudad de Jaén", 23007 Jaén, Spain; vazquez89@arrakis.es
6 Department of Pharmacology, School of Medicine, Complutense University of Madrid, 28040 Madrid, Spain;
   edelpon@med.ucm.es (E.D.); rcaballero@med.ucm.es (R.C.)
* Correspondence: leif.hove@iibb.csic.es; Tel.: +34-935-565-620; Fax: +34-935-565-603
† Contributed equally to this work.
‡ Co-senior authors.

Abstract: Atrial fibrillation (AF) is the most common cardiac arrhythmia in the human population, with an estimated incidence of 1–2% in young adults but increasing to more than 10% in 80+ years patients. Pituitary Homeobox 2, Paired Like Homeodomain 2 (PITX2c) loss-of-function in mice revealed that this homeodomain (HD)-containing transcription factor plays a pivotal role in atrial electrophysiology and calcium homeostasis and point to PITX2 as a candidate gene for AF. To address this issue, we recruited 31 AF patients for genetic analyses of both the known risk alleles and PITX2c open reading frame (ORF) re-sequencing. We found two-point mutations in the homedomain of *PITX2* and three other variants in the 5'untranslated region. A 65 years old male patient without 4q25 risk variants but with recurrent AF displayed two distinct HD-mutations, NM_000325.5:c.309G>C (Gln103His) and NM_000325.5:c.370G>A (Glu124Lys), which both resulted in a change within a highly conserved amino acid position. To address the functional impact of the PITX2 HD mutations, we generated plasmid constructs with mutated version of each nucleotide variant (MD4 and MD5, respectively) as well as a dominant negative control construct in which the PITX2 HD was lacking (DN). Functional analyses demonstrated PITX2c MD4 and PITX2c MD5 decreased Nppa-luciferase transactivation by 50% and 40%, respectively, similar to the PITX2c DN (50%), while Shox2 promoter repression was also impaired. Co-transactivation with other cardiac-enriched co-factors, such as Gata4 and Nkx2.5, was similarly impaired, further supporting the pivotal role of these mutations for correct PITX2c function. Furthermore, when expressed in HL1 cardiomyocyte cultures, the PITX2 mutants impaired endogenous expression of calcium regulatory proteins and induced alterations in sarcoplasmic reticulum (SR) calcium accumulation. This favored alternating and irregular calcium transient amplitudes, causing deterioration of the beat-to-beat stability upon elevation of the stimulation frequency. Overall this data demonstrate that these novel PITX2c HD-mutations might be causative of atrial fibrillation in the carrier.

Keywords: atrial fibrillation; PITX2 mutations; sarcoplasmic reticulum; calcium imaging; cardiomyocyte culture

1. Introduction

Atrial fibrillation (AF) is the most common cardiac arrhythmia in the human population, with an estimated incidence of 1–2% in young adults but increasing to more than 10% in 80+ years patients [1]. Thanks to genome wide association studies (GWAS) an increasing number of single nucleotide polymorphisms (SNPs) have been associated with risk of AF [2–5] with some of the most significant are located in 4q25 locus. Given the key developmental role of Pitx2 during cardiogenesis [6,7], and particularly its role in pulmonary vein formation [8], it has been postulated that PITX2c dysfunction might be responsible for AF [2]. Experimental evidence in distinct laboratories, including ours, have demonstrated that PITX2c loss of function predisposes to atrial arrhythmogenesis [9–12] and provokes disturbances in the calcium homeostasis [13]. In line with this, the 4q25 risk variant rs13143308 has recently been linked to defective calcium homeostasis [14], pointing to *PITX2* as a candidate gene for AF.

Mutations in the homeobox transcription factor2 gene have been linked to Axenfeld Rieger syndrome [15–19], distinct ocular defects [20–22] and congenital heart defects [23]. Given the complexity of the ocular, facial and cardiac phenotypes revealed by PITX2c loss-of-function in mice and man, it was suggested that *PITX2* mutations could be underlying CHARGE syndrome but direct sequencing of 29 affected individuals did not reveal any mutation [24]. However, several papers have identified novel mutations in the PITX2 homedomain associated with AF [25–30], with some of them impairing their transactivation capacity of the Nppa basal promoter [31], as a downstream target of PITX2c as previously demonstrated [32,33].

In this study we have searched for mutations in AF patients in a small cohort of 31 patients with distinct degrees of AF; sporadic, recurrent and permanent. Assessment of known 4q25 AF risk variants (rs2200733, rs13143308, rs10033464) was run in parallel with direct DNA sequencing of the *PITX2* open reading frame (ORF). We have identified two-point mutations in the homeodomain of PITX2 and three polymorphisms in the 5´untranslated region. To test if these novel PITX2 HD point mutations could underlie the onset of atrial fibrillation in this patient, we assessed their functional impact on transactivation of both reported constructs, on endogenous calcium regulatory genes, and on calcium homeostasis and beat-to-beat stability in transfected cardiomyocyte cultures. Functionally, both mutations impaired Nppa transactivation and Shox2 repression as well as endogenous calcium regulatory gene expression. This in turn deteriorated the calcium homeostasis and beat-to-beat stability in transfected cardiomyocyte cultures.

2. Methods

2.1. Patient Recruitment and Sample Collection

Patients referred to the Cardiology Unit of the Regional Hospital in Jaen, during a 24-month period, with a recorded history of atrial fibrillation or de novo assessment of paroxysmal AF were included in the study. Informed consent was obtained in all cases. Peripheral blood samples were collected from all enrolled patients in EDTA tubes and stored at -20 °C until DNA extraction was carried out. Control genomic DNAs were obtained from the Spanish DNA National Bank (Banco Nacional de ADN, Salamanca, Spain). Genomic DNA from all participants was extracted from blood lymphocytes with Wizard Genomic DNA Purification Kit (Promega; Madison WI, USA).

2.2. DNA Sequencing

Mutations of the *PITX2* gene (NM_000325) were screened according to the following method. Each *PITX2* exon and their splice sites were amplified by polymerase chain reaction (PCR) using intronic PCR primers as detailed in Table 1. For all PCR, genomic DNA (100 ng) was amplified using a Mastercycler personal thermal cycler (Eppendorf, Hamburg, Germany) in 25 μL reaction mixture containing 1.5 mM $MgCl_2$, 1 mM of each primer, 0.2 mM deoxyribonucleoside triphosphate, and 0.5 IU of GoTaq_Flexi DNA polymerase (Promega, Madison, WI, USA). The resulting reaction mixtures were purified using

the Genomics Millipore Montage® PCR Centrifugal Filter Device (Millipore Corporate Headquarters, Billerica, USA) the PCR products were sequenced (Sistemas Genómicos, Valencia, Spain). Chromatogram files were processed using Chromas Pro 2.33 software (Technelysium Pty Ltd.) and Blast (www.ncbi.nlm.nih.gov). Sequence alignments with the reference *PITX2* gene (NM_000325) were performed. In case of abnormality detection, PCR amplification and re-sequencing was repeated at least three times for further validation. Variants were described using the Human Genome Variation Society guidelines (http://www.varnomen.hgvs.org, accessed on 1 March 2020) for nomenclature [34].

Table 1. Primer sequences used for human PITX2 sequencing and for site-directed mutagenesis.

Sequencing	Forward Primers	Reverse Primers
1	5′ AGATTTCAGAGGGCCCAGAT 3′	5′ CGACCTCCTTCCTTTTGCTT 3′
2	5′ GGCACACTTTTCGAGTGAGA 3′	5′ CCAAGAGACGGAACAAAGGA 3′
3	5′ CTCACACCCACACTCCACAC 3′	5′ ATTCCACCAAACTCCACTGC 3′
4	5′ CTCCCCTGCCTCGTTTCT 3′	5′ GGGATAGATGGCCTCCACTT 3′
5	5′ CGAACAGACATCTCAATCAGG 3′	5′ GGTGGGAGCAAGCGTTGT 3′
6	5′ AGTCTCATCTGAGCCCTGCT 3′	5′ CTGGCGATTTGGTTCTGATT 3′
7	5′ TGGGTCTTTGCTCTTTGTCC 3′	5′ CTTCCCTCCCGGCCTTAC 3′
8	5′ CCCGCCTCTGGTTTTAAGAT 3′	5′ AAAGTCCGGAGACGGAAAGT 3′
9	5′ CTTGTTTCGCTTTGGAGCTT 3′	5′ AGGGGCTGACTTCCTTGG 3′
10	5′ ATGCTGACGGGAAAGTGTGT 3′	5′ GGCCTGTACCTCCACAACAT 3′
11	5′ GCATCTGTTTGCTCCCTTG 3′	5′ GACGGGCTACTCAGGTTGTT 3′
12	5′ ATGAGCATGTCGTCCAGCAT 3′	5′ TGAAAGATGTCAGACACTGAGGA 3′
13	5′ GAAAAGGAAACCACTGAATCAAA 3′	5′ TGTTAGAAACATACAGTGTGGCATT 3′
14	5′ CAACAGTGTTTTTAAAGGTTAGGC 3′	5′ AGGAGGGGAGAAAGAATCCA 3′
Mutagenesis	Forward Primers	Reverse Primers
G947C (Gln103His)	5′acttaccagccagcaCctccaggagctggagg 3′	5′cctccagctcctggagGtgctggctggtaaagt 3′
G1008C (Glu124Lys)	5′catgtccacacgcgaaCaaatcgctgtgtggac 3′	5′gtccacacagcgatttGttcgcgtgtggacatg 3′

Pathogenicity of unreported variants was assessed by evaluating their absence in at least 100 control chromosomes, in 1000 genomes (http://browser.1000genomes.org, accessed on 1 February 2020) and Exome Sequencing Project (http://evs.gs.washington.edu/EVS/, accessed on 1 February 2020) databases. In addition, variants were classified as potentially damaging protein function using in silico prediction software such as MutationTaster (http://www.mutationtaster.org/, accessed on 1 February 2020) and Polyphen 2 (http://genetics.bwh.harvard.edu/pph2/, accessed on 1 February 2020) and as pathogenic based on the American College of Medical Genetics and Genomics [12] and the European Society of Human Genetics classification (https://www.eshg.org/fileadmin/www.eshg.org/documents/Variant_classification_system/Variant_class_ESHG.pdf, accessed on 1 February 2020).

2.3. Generation of Reporter and Mutated PITX2c Constructs

Rat atrial natriuretic factor (ANF; *Nppa*) promoter sequence [35,36] was amplified from rat genomic DNA with specific primers bearing EcoRI/ BamHI restriction sites (Forward: TGTAGCTGAATTCTTTAGAGCCTGT; Reverse: GGGGGATCCGATCTGATGTTTGCTGTCTC) and cloned into pGLuc-Basic vector (New England Biolabs). V5-Tag-pcDNA3.1/Zeo vector was created as previously described [37]. The *PITX2* ORF was amplified from mouse muscle cDNA with specific primers bearing XbaI/NotI restriction sites (Forward: CCCTCTAGAATGAACTGCATGAAAG; Reverse: GGGGCGGCCGCACACCGGCCGGTCG) and cloned in V5-Tag-pcDNA3.1/Zeo vector in frame with C-terminal V5 epitope, creating Pitx2_V5-Tag-pcDNA3.1/Zeo vector.

The human PITX2C ORF was amplified from human muscle cDNA with specific primers bearing BamHI/AgeI restriction sites (Forward: CCCGGATCCATGAACTGCATGAAAGG; Reverse: CCCACCGGTCACGGGCCGGTCC) and cloned in pcDNA3.1/V5-His-TOPO vector (Life Technologies) removing V5 epitope and in frame with the C-terminal

His tag epitope, creating pcDNA3.1 PITX2C-His-TOPO vector. To generate a vector able to code for the human PITX2c protein without the homeodomain (HD) sequence, PITX2C ORF fragment ranging from nucleotides 1 to 276 was amplified from pcDNA3.1 PITX2C-His-TOPO vector with specific primers bearing NheI/BamHI restriction sites (Forward: CC-CGCTAGCATGAACTGCATGAAAGG; Reverse: CCCGGATCCTTGCCGCTTCTTCTTA) and cloned in pcDNA3.1 Zeo(-) vector (Life Technologies). After this, PITX2C ORF fragment ranging from nucleotides 454 to 972 in frame with His tag was amplified from pcDNA3.1 PITX2C-His-TOPO vector with specific primers bearing BamHI/HindII restriction sites (Forward: CCCGGATCCCGCAACCAGCAGGCCG; Reverse: CCCAAGCTTTCAATGGT-GATGGTGATG) and cloned in the same pcDNA3.1 Zeo(-) creating pcDNA3.1 PITX2C-DN-His-TOPO vector. This construct codifies a human recombinant PITX2C protein without the sequence ranging from amino acid 92 to 151, corresponding the PITX2C homeodomain, i.e., PITX2C DN construct.

The identified mutation was introduced into the wild-type PITX2c construct using an iProof High Fidelity DNA polymerase (BioRad, Hercules, CA, USA) with a complementary pair of primers. The mutant was sequenced to confirm the desired mutation and to exclude any other sequence variations.

PCR-based site-directed mutagenesis was performed using Stratagene QuikChange Site-Directed Mutagenesis kit, but using the enzymes and buffers from the Bio-Rad iPROOF PCR kit. Amplification conditions were: 98 °C for 60 s followed by 14 cycles of 98 °C for 10 s, 55 °C for 30 s and 72 °C for 6 min followed by 72 °C for 10 min. All cloning PCRs were performed by using iProof High-Fidelity DNA Polymerase (Bio-Rad). Amplification conditions were: 98 °C for 30 s followed by 35 cycles of 98 °C for 10 s, 64 °C for 30 s and 72 °C for 2 min followed by 72 °C for 10 min.

2.4. Cell Culture and Luciferase Transactivation Assays

Mouse fibroblast (3T3) cells were grown in Dulbecco's modified Eagle's medium supplemented with 10% fetal bovine serum, 200 mM L-Glu as well as 1000 units/mL penicillin and 10 µg/mL streptomycin. 3T3 cells were cultured 24 h prior transfection. The rat *Nppa*-pGluc reporter and the mouse Shox2-pGluc reporter constructs [11], with the corresponding internal control reporter plasmid psV40-pCluc were used in transient transfection assays to explore the transactivation activity of different PITX2c constructs, alone or in distinct combinations. Briefly, 3T3 cells were transfected with either 400 ng of wild-type PITX2c-pcDNA, PITX2cDN-pcDNA, the corresponding mutant PITX2c-pcDNA construct (MD4, carrying Gln103His mutation; MD5 carrying Glu124Lys mutations; MD4+5 carrying both Gln103His and Glu124Lys mutations), 400 ng of *Nppa*-pGluc reporter construct and 100 ng of psV40-pCluc control reporter vector using Lipofectamine 2000 Transfection Reagent (Invitrogen, Carlsbad, CA, USA). In addition, co-transfection experiments with Gata4, Nkx2.5 or both expression vectors was performed as previously reported [38]. Transfected cells were incubated for 24 h and cell culture supernatant were harvested and assayed for reporter activities. Cypridina luciferase and Gaussia luciferase activities were measured with the BioLux Cypridina Luciferase Assay Kit and BioLux Gaussia Luciferase Assay Kit (NEBL). The activity of the promoter was presented as fold activation of Gaussia luciferase relative to Cypridina luciferase. Three independent experiments were performed at minimum for each experimental condition and the corresponding mean and standard deviation error are represented.

HL-1 cells (6×10^5 cells per well) were transfected described above with increasing doses of PITX2c mutant constructs and the wild type PITX2c construct to assess the endogenous transcript expression (ion channels and transcription factors). A 1:1, 1:2 and 1:4 ratio (wt vs. mutant) was assayed and further processed of RNA isolation. Similarly as detailed above, three independent experiments were performed and the corresponding mean values and standard deviation errors were plotted.

In addition to test the rat *Nppa* and mouse *Shox2* promoter, the basal human *NPPA* promoter was also assayed in HL1 cardiomyocytes. HL-1 cells were seeded in 96-well plates

and cultured as described above. Cells were transfected with the proximal *NPPA* promoter cloned into pLightswitch vector (100 ng; Active Motif, Carlsbad, CA, USA), which contains firefly luciferase as a reporter. Moreover, an empty vector, WT, a dominant negative or mutants of PITX2c were co-transfected (50 ng). All transfections were performed by using Lipofectamine 2000 (Invitrogen) according to the manufacturer's instructions. Luciferase activity assays were performed 24 h after transfection using the LightSwitch™ Luciferase Assay Kit (Active Motif, Carlsbad, CA, USA) and a Berthold Luminometer. Luciferase activity was normalized to sample protein concentration. All reporter assays were performed in triplicate.

2.5. qRT-PCR Analyses

Transfected cells were collected and total RNA from cultured 3T3 cells was extracted with the TriPure isolation reagent (Roche Diagnostics, Rotkreuz, Switzerland), treated with RNase-free DNase (Roche) for 1 h at 37 °C and purified using a standard phenol–chloroform protocol. RNA yield and purity was determined spectrophotometrically, and RNA integrity was verified by running samples on 1.2% agarose gels and staining with ethidium bromide. Resulting RNA preparations were resolved in nuclease-free water and kept at −80 °C. One microgram aliquots of individual total RNA were reverse transcribed using Maxima First Strand cDNA Synthesis Kit for RT-qPCR (Thermo Scientific) according to the manufacturer's instructions. Negative control reactions were performed in the same conditions without reverse transcriptase.

All qRT-PCR experiments followed MIQE guidelines [39]. Transcript (mRNA) real time PCR experiments were performed with 1 μL of cDNA, SsoFast EvaGreen mix and corresponding primer sets as described on Table 2. All qPCRs were performed using a CFX384TM thermocycler (Bio-Rad) following the manufacturer's recommendations. The relative level of mRNA synthesis was calculated as described by Livak and Schmittgen [40] using housekeeping genes coding for glyceraldehyde-3-phosphate dehydrogenase (Gapdh) and β-D-glucuronidase (Gusb) as internal controls. Each PCR reaction was carried out in triplicate and repeated in at least three distinct biological samples to obtain representative means.

Table 2. Primer sequences used for qPCR in HL-1 cardiomyocyte cultures.

Gene	Forward Primers	Reverse Primers
Mm Gapdh	5′ TCTTGCTCAGTGTCCTTGCTGG 3′	5′ TCCTGGTATGACAATGAATACGC 3′
Mm Gusb	5′ ACGCATCAGAAGCCGATTAT 3′	5′ ACTCTCAGCGGTGACTGGTT 3′
Mm Atp2a2	5′ TGGGAGAATATCTGGCTCGT 3′	5′ AGGCAAGGAGATTTTCAGCA 3′
Mm Pln	5′ ATGCTCTGCACTGTGACGAT 3′	5′ TTTCCATTATGCCAGGAAGG 3′
Mm Casq1	5′ CCCGTACTGGGAGAAGACCT 3′	5′ CAGGTCCTCCTCGTTATCCA 3′
Mm Nkx2.5	5′ AGGTACCGCTGTTGCTTGAA 3′	5′ CAAGTGCTCTCCTGCTTTCC 3′
Mm Gata4	5′ GCAGCAGCAGTGAAGAGATG 3′	5′ GCGATGTCTGAGTGACAGGA 3′

2.6. Intracellular Calcium Recordings in HL-1 Myocytes

Cultured atrial HL-1 myocytes used for calcium imaging experiments were expanded and maintained in a Claycomb Medium (JRH Biosciences, Lenexa, KS, USA) supplemented with 10% fetal bovine serum (FBS) (Invitrogen Corporation, Carlsbad, CA, USA), 100 μM norepinephrine, 100 units/mL penicillin, 100 μg/mL streptomycin, and L-Glutamine 2 mM (Sigma Chemical Company, St. Louis, MO, USA) in plastic dishes, coated with 12.5 μg/mL fibronectin and 0.02% gelatin, in a 5% CO_2 atmosphere at 37 °C. HL-1 cells were transfected as described above with PITX2c mutant constructs or the wild type PITX2c construct to assess the impact on intracellular calcium homeostasis. Two days after transfection, cultures were transferred to norepinephrine-free Tyrode solution containing (in mM): NaCl 136, KCl 4, NaH_2PO_4 0.33, $NaHCO_3$ 4, $CaCl_2$ 2, $MgCl_2$ 1.6, HEPES 10, Glucose 5, pyruvic acid 5, (pH = 7.4) and left for at least three hours before calcium imaging was performed. The experimental protocol consisted in field stimulation of the myocyte cultures at 2x the voltage necessary for eliciting a full calcium transient. The stimulation frequency was

gradually increased from 0.5 to 1, 1.3, 2 and 4 HZ at intervals allowing the calcium transient to reach steady-state at each stimulation frequency.

To visualize changes in the intracellular calcium concentration, HL-1 cultures were loaded with 2 μM Cal-590 for 20 min, followed by at least 30 min wash and de-esterification. Confocal calcium images of 512×512 pixels were recorded at room temperature at a frame rate of 30 Hz with a resonance-scanning confocal microscope (Leica SP5 AOBS) and a HCX PL APO CS 20.0×0.70 IMM UV objective. Cal-590 was excited at 543 nm and fluorescence emission collected between 570 and 750 nm. Laser power was set to 20% of 1 mW and then attenuated to 6% (of the 20%). Fluorescence emission was measured with a Leica Hybrid detector in standard mode with a gain of 30%. Several image fields were recorded in each culture dish. Transfection with the different PITX2c constructs was successfully done in 9 different HL1 cultures. Non-confluent myocyte cultures with low cell density and cultures with poor calcium transients in reference conditions (WT or pcDNA) were discarded.

Image analysis was performed using a custom made program that allowed identification of myocytes with a detectable calcium signal and the beat-to-beat response in the whole image field and in individual myocytes with calcium signals as previously described [41]. Briefly, this program identifies all myocytes with calcium transients and assigns them a number. Subsequently, calcium transients from each myocyte is analyzed and features such as amplitude, duration, and decay time were determined at 0.5 Hz where preparations present a uniform response. In this condition, the error of the measurement of the full duration of the calcium transient at half maximum is less than 7%. The beat-to-beat response is determined by an algorithm based on expert classification of the beat-to-beat response at stimulation frequencies ranging from 0.2 to 4 Hz in more than 1000 individual myocytes from image fields recorded in at least 10 different HL-1 cultures. Unless otherwise stated, whole field responses were analyzed to achieve optimal signal to noise ratio and best signal classification responses were separated into the following categories: Uniform response; alternation of the amplitude with the extreme case being blockade where every second, 2 of 3 or 3 of 4 transients were suppressed; Irregular response; and calcium waves, a response where response to field stimulation was interrupted by spontaneous calcium waves with a duration that extended across several stimulation pulses.

2.7. Statistical Analysis

Values presented are expressed as mean $\pm$ S.E.M. All comparisons between groups were performed using an unpaired Student's t test or Wilcoxon's rank test for data that did not have a normal distribution. ANOVA was used for multiple comparisons of normally distributed data. Differences were considered statistically significant for p value ≤ 0.05.

3. Results

3.1. Mutation Screening of PITX2c Reveals in AF Patients Revealed Two Novel HD Mutations

PITX2 has been recently associated as candidate gene to underlay AF by GWAS. We have conducted a genetic screening on the *PITX2* ORF (NM_000325_5) in 31 patients diagnosed with AF according to the ESC Guidelines for treatment of AF referred to the Cardiology Unit of the Regional Hospital "Ciudad de Jaen". Male patients represented 77% of the enrolled cases. Hypertension was diagnosed in 45% of all patients while type II diabetes was found in 19% of the cases. Among all AF patients 7/31 (~22,5%) were diagnosed as having paroxysmal AF, 10/31 (~32%) had recurrent AF and 12/31 (~39%) permanent AF. The remaining two (2/31; ~6,5%) had just shown the first episode of AF. After informed consent was obtained from each patient, a peripheral blood sample was obtained and processed for DNA isolation using standard procedures. Genetic screening of the *PITX2* coding sequence identified two nucleotide substitutions at NM_000325.5:c.309G>C. (Gln103His) and NM_000325.5:c.370G>A (Glu124Lys), respectively, corresponding to distinct amino acids forming part of the homeodomain region of the PITX2c transcription factor (Figure 1A). Importantly, these nucleotide changes lead to amino acid substitution Gln103His and Glu124Lys, respectively. Comparative analyses of the conservation of Gln103His and

Glu124Lys demonstrate that these amino acids are highly conserved in different species, increasing thus the likelihood that they might be detrimental (Figure 1B). Both variants were classified as potentially damaging PITX2c protein function using in silico prediction software MutationTaster (http://www.mutationtaster.org, accessed on 1 February 2020). Both NM_000325.5:c.309G>C. (Gln103His) and NM_000325.5:c.370G>A (Glu124Lys) variants were absent in the control populations of both Exome and 1000 genome projects (https://www.internationalgenome.org/1000-genomes-browsers/, accessed on 1 February 2020). Curiously, both variants were identified in a 65 years old male patient with recurrent AF who did not carry any 4q25 risk variants corresponding at any of the rs2200733, rs13143308 or rs10033464 SNPs.
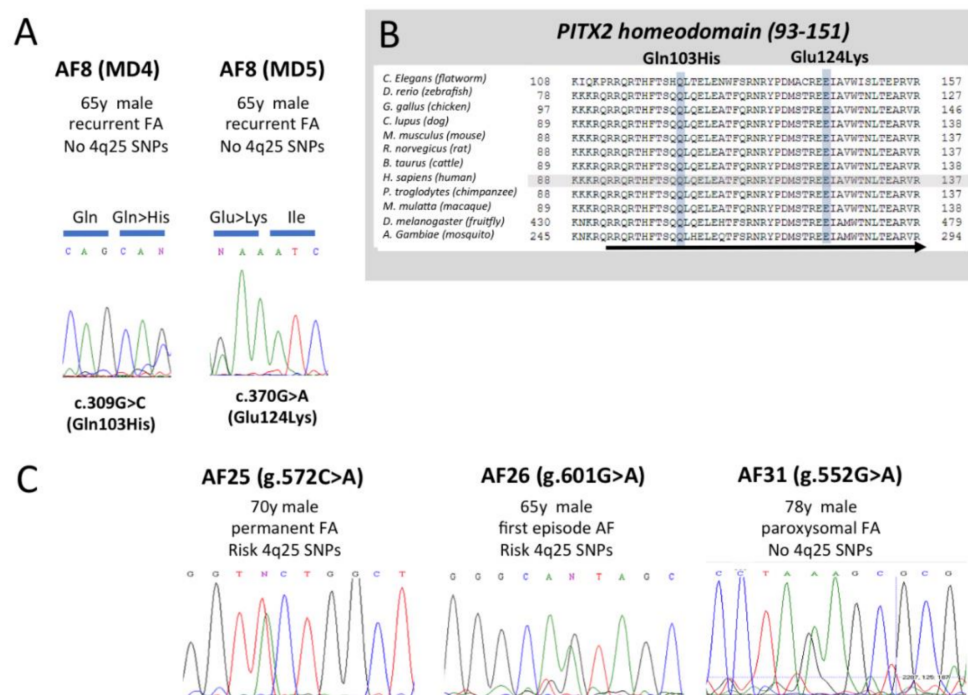

Figure 1. Pitx2 mutations in atrial fibrillation patients. Panel (**A**). Representative chromatograms of c.309G>C (Q1103H) and c.370G>A (Glu124Lys) mutations in the PITX2 homeodomain identified in a AF patient. Panel (**B**). Comparative alignment of the PITX2 homeodomain region illustrating the conserved amino acid position of these identified mutations in different species. Panel (**C**). Representative chromatograms of cDNA.582C>A, cDNA.601G>A and cDNA.552G>A mutations in the PITX2 5 untranslated region identified in distinct AF patients.

In addition to these two nucleotide substitutions, three additional nucleotide substitutions were identified in the 5´untranslated region of the PITX2c transcription factor (Figure 1C), corresponding to the following positions: NM_000325.5:g.572C>A, NM_000325.5:g.601G>A and NM_000325.5:g.552A. C572A nucleotide substitution was identified in a 70 years old male patient with permanent FA, type II diabetes but no hypertension and with the presence of risk variants at rs13143308 and rs10033464 but not at rs2200733. G601A was identified in a 65 years old male patient with the first episode of AF, without hypertension or type II diabetes. Risk variants at rs13143308 and rs2200733 but not at rs10033464 were identified in this patient. Finally, G552A variant was identified in a 78 years old male AF patient with paroxysomal AF, hypertension but not type II diabetes. This patient carried no risk variants for any of the three AF-associated SNPs. NM_000325.5:g.601G>A and NM_000325.5:g.552A variants, but no NM_000325.5:g.572C>A, were classified as potentially damaging PITX2c protein function (plausible splice site alterations) using in silico MutationTaster prediction software.

3.2. Gln103His and Glu124Lys Mutations Impairs PITX2c Transactivation Activity

In order to test if the identified nucleotide substitutions in the homeodomain of the PITX2c transcription factor have a functional impact, we constructed site-directed mutants carrying the corresponding Gln103His and Glu124Lys mutations alone or in combination. In addition, we also engineered a dominant-negative PITX2c (DN) mutant by selective deletion of the homeodomain region. Co-transfection of these plasmids with the rat Nppa-pGLuc construct demonstrated that wild-type PITX2c is capable of transactivating 5 fold the Nppa basal promoter, in line with previous reports [32,33], while PITX2c DN reduced by half such transactivation capacity (Figure 2A). Importantly, constructs carrying Gln103His (MD4) and Glu124Lys (MD5) mutations lead to 50% and 40% reduction in the transactivation capacity, respectively. Interestingly, PITX2c constructs carrying both mutations (MD4+5) display similar impaired transactivation capacity of the Nppa-pGLuc promoter as those carrying individual mutations.

To add further support to this data, we conducted luciferase gene expression reporter assays by using HL-1 cells transfected with the proximal promoter region of the human atrial natriuretic peptide. Transfection of PITX2c WT (50 ng) resulted in a 2.5-fold increase of the luciferase activity compared to that measured in the presence of an empty vector (Control) (Figure 2B). The specificity of the PITX2c effect was supported by the absence of changes produced by the PITX2c dominant negative. Interestingly, MD4, MD5 or MD4+5 constructs failed to modify luciferase activity confirming that these are loss-of-function mutations.

To further validate the transcriptional impairment of these novel PITX2 HD mutations, we performed co-transfection assays using the Shox2 promoter (Figure 2C). As previously reported, wild-type PITX2c over-expression represses the Shox2 promoter [11]. Interestingly, both Gln103His (MD4) and Glu124Lys (MD5) mutations leads to enhanced activation of the Shox2 promoter as compared to wild type PITX2c co-transfections, which is more pronounced for the MD5 as compared to MD4 constructs. In line with these findings, double mutants (MD4+5) display similar transactivation properties as the MD5 construct.

The *Nppa* promoter is modulated not only by PITX2c but also by other cardiac-enriched transcription factors, such as Gata4 and Nkx2.5 [33]. We therefore tested if Gln103His and Glu124Lys mutations also impaired the synergistic transactivation of PITX2c with these transcription factors (Figure 2D–F). Co-transfection experiments demonstrate that Gln103His and Glu124Lys mutations impaired *Nppa* promoter transactivation within a similar range. Interestingly, double mutants also displayed similar transactivation impairment in both conditions, when co-transfected with either Nkx2.5 or Gata4.

Overall these data suggest that both novel *PITX2* mutations alter the transactivation properties of PITX2c similarly when acting as a transcriptional activator, whereas some differences occur in cases where PITX2c acts as a transcriptional repressor. Furthermore, these assays indicate that no synergistic effects are observed by the presence of both mutations within the same gene.

3.3. Gln103His and Glu124Lys PITX2 Mutations Alter Calcium Homeostasis

To further investigate if these novel PITX2 mutations can impair endogenous expression levels and function of PITX2 downstream genes, we performed co-transfection assays of wild-type PITX2c with distinct doses of the mutated PITX2c constructs within HL-1 atrial cardiomyocytes. We have previously reported that PITX2c impairment in mice leads to changes in ion channel expression and calcium homeostasis and we therefore used confocal calcium imaging in HL1 myocyte cultures to test how the mutated PITX2c constructs affect the properties and stability of the calcium transients elicited by electrical field stimulation.
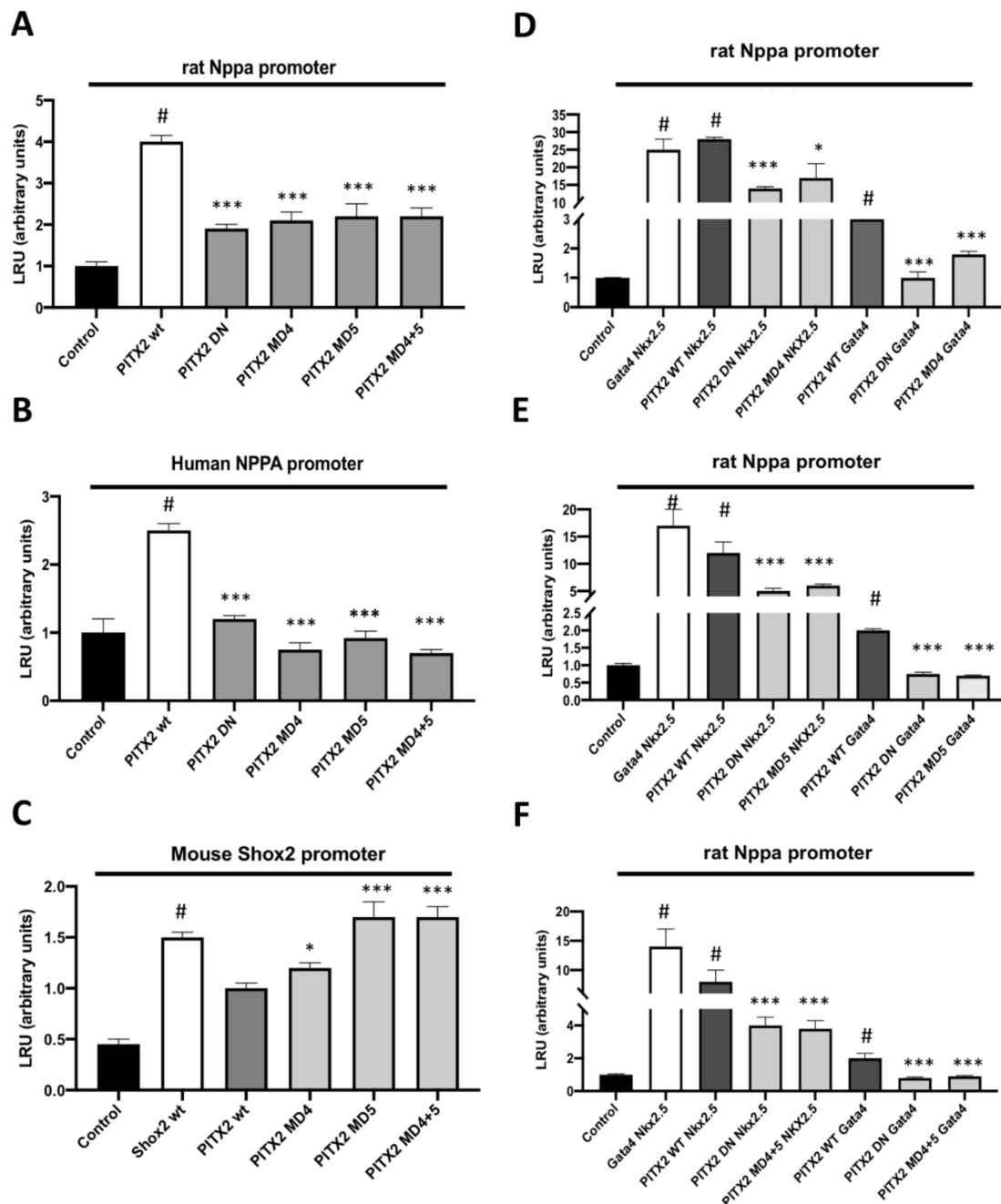
Figure 2. Pitx2 transactivation assays. Panel (**A**). PITX2 transactivation assays of the PITX2 wild type, DN, MD4, MD5 and MD4+5 constructs within the rat *Nppa* promoter. Observe that PITX2c wild type significantly enhanced luciferase expression as compared to controls, while PITX2 DN, MD4, MD5 and MD4+5 constructs significantly decreased their transactivation as compared to PITX2c wild type. Panel (**B**). PITX2 transactivation assays of the PITX2 wild type, DN, MD4, MD5 and MD4+5 constructs within the human *Nppa* promoter. Observe that PITX2c wild type significantly enhanced luciferase expression as compared to controls, while PITX2 DN, MD4, MD5 and MD4+5 constructs significantly decreased their transactivation as compared to PITX2c wild type. Panel (**C**). PITX2 transactivation assays of the PITX2 wild type, DN, MD4, MD5 and MD4+5 constructs within the mouse *Shox2* promoter. Observe that PITX2c wild type significantly repressed luciferase expression as compared to Shox2 controls, while PITX2 MD4, MD5 and MD4+5 constructs significantly enhanced their transactivation as compared to PITX2c wild type transfections. Co-transfections assays of PITX2c and cardiac enriched transcription factors Nkx2.5 and Gata4 respectively, demonstrate that PITX2c MD4 (panel (**D**)), PITX2c MD5 (panel (**E**)) and PITX2c MD4+5, significantly impaired their transactivation capacity on the rat *Nppa* promoter (panel (**F**)). Experiments were carried out in triplicate and repeated in at least three distinct biological samples. # $p < 0.05$ statistical significance as compared to controls. * $p < 0.05$, *** $p < 0.001$ statistical significance as compared to corresponding PITX2c WT conditions.

In the first set of experiments, the effects of several PITX2c constructs on the intracellular calcium transients were examined in HL-1 cardiomyocyte cultures. Transients were examined in cultures transfected with control (pcDNA), MD4, MD5, MD4+5 or DN PITX2c mutants. Figure 3A shows a 450 × 450μm field of HL-1 myocytes co-transfected with GFP (left panel). The intracellular calcium level was monitored simultaneously using the fluorescent calcium indicator Rhod-2 (central panel) and the overlay of the two channels are shown on the right. Calcium transients recorded at different stimulation frequencies are shown in Figure 3B. Because the PITX2c mutants affected the beat-to-beat stability, calcium transient properties were evaluated at 0.5 Hz, where all preparations responded to the electrical pulses. Figure 3C shows that while the calcium transient amplitude tended to decrease for the PITX2c mutants, the reduction was only significant for the MD5 and the DN mutant. The calcium transient duration at half maximum was not significantly affected by any of the mutants (Figure 3D).
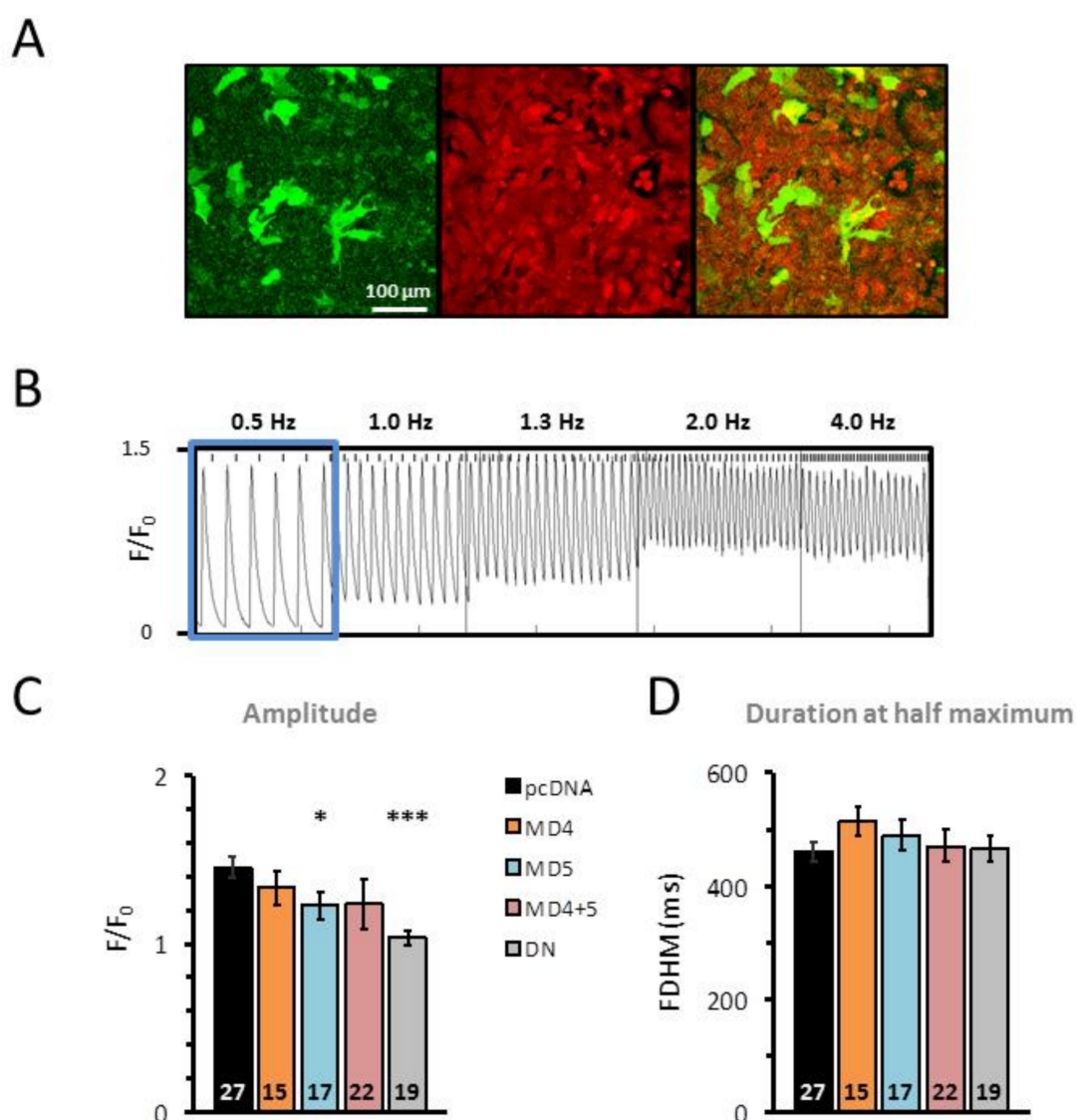

Figure 3. Impact of Pitx2 mutations on calcium transients. Panel (**A**). Images of a HL1 myocyte culture co-transfected with GFP and pcDNA (left). The middle panel shows calcium imaging of the same culture and the right panel shows these two images superimposed. Panel (**B**). Calcium transients recorded at increasing stimulation frequencies from the image field shown in panel A. Calcium transient properties were measured at 0.5 Hz where all preparations responded to electrical field stimulation. Panel (**C**). Calcium transient amplitude in HL1 cultures transfected with pcDNA, MD4, MD5, MD4+5 or DN Pitx2 constructs. Panel (**D**). Duration of the calcium transients at half maximum. Number of experiments is given for each bar. Values significantly different from pcDNA are indicated with * $p < 0.05$; *** $p < 0.001$.

To test if differences in the calcium transient amplitude were caused by alterations in SR calcium homeostasis, we first used a rapid caffeine application to release the SR calcium content into the cytosol. Figure 4A, shows the caffeine induced calcium transient and Figure 4B compares the peak amplitude for the different PITX2c constructs. Interestingly, all PITX2 mutants except the MD4 mutant displayed reduced SR calcium content compared with controls (pcDNA). These differences did not appear to be related to differential modulation of the Serca2 (Atp2a2) or phospholamban (Pln) mRNA levels by the different PITX2 mutants since there was a robust and parallel down-regulation of both Serca2 and Pln levels for MD4, MD5 and MD4+5 (Figure 4C–E), suggesting that the calcium-dependency of the uptake rate is unaffected by the mutants while the maximal uptake rate may be blunted in all three mutants. Interestingly, the SR calcium buffering protein, calsequestrin (Casq2), was also reduced by more than 50% in the MD4+5 mutant (Figure 4E).
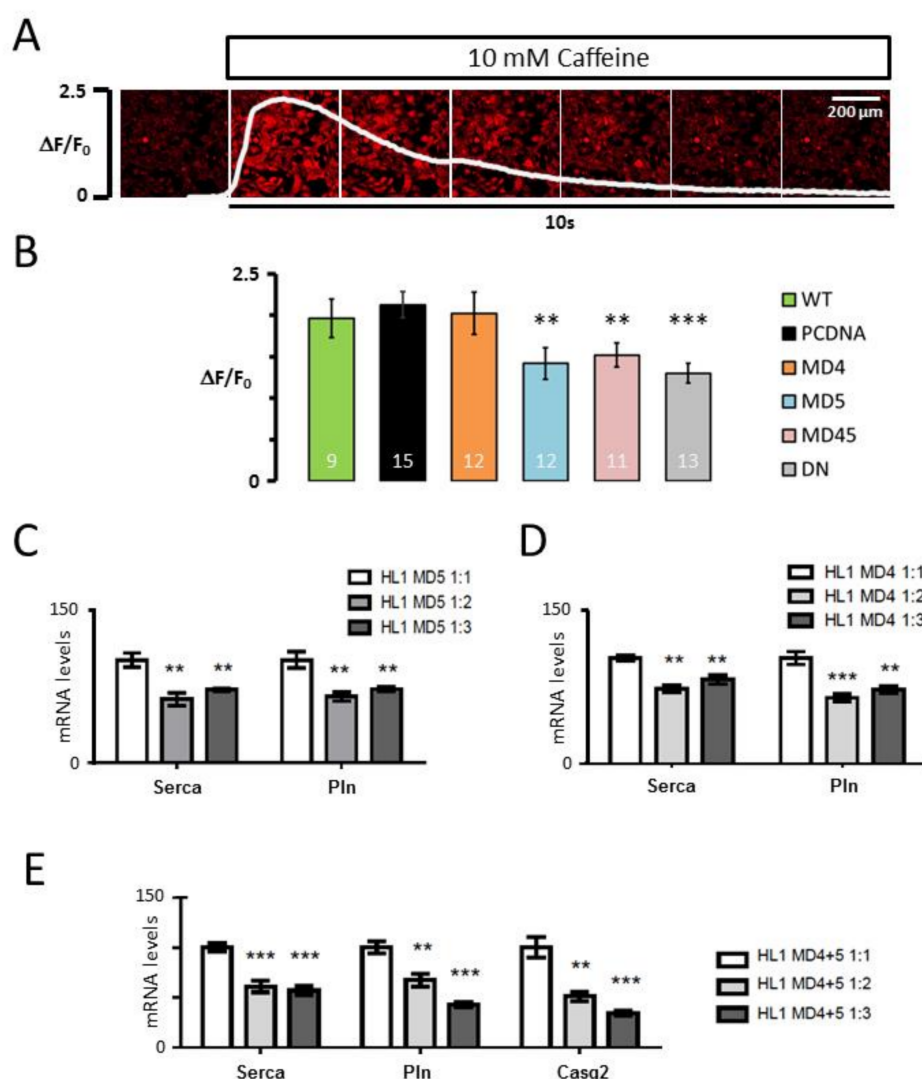

Figure 4. Impact of Pitx2 mutations on SR calcium homeostasis. Panel (**A**). Images recorded during rapid application of 10 mM caffeine with quantification of the resulting transient increase in the calcium signal superimposed. Panel (**B**). Amplitude of the calcium transient peak induced by caffeine in HL1 myocyte cultures transfected with WT, pcDNA, MD4, MD5, MD4+5 or DN constructs. Number of experiments is given for each bar. Transfection of HL1 cardiomyocytes with MD5 (Panel (**C**)) and MD4 (Panel (**D**)) reduces Serca and Pln mRNA levels. Panel (**E**). Transfection of HL1 cardiomyocytes with MD5 reduces Serca, Pln and Casq mRNA levels. Experiments were carried out in triplicate and repeated in at least three distinct biological samples. Values significantly different from the reference condition are indicated with ** $p < 0.01$; *** $p < 0.001$.

3.4. Impact of Gln103His and Glu124Lys PITX2c Mutations on the Beat-to-Beat Response

While these alterations in the SR calcium content and calcium transient amplitude are expected to modulate shortening of the cardiomyocytes, these features may also affect the beat-to-beat response when the stimulation frequency is increased. As shown in Figure 5 a stepwise increase in the stimulation frequency from 0.5 to 4 Hz modified the calcium transients in the whole image field (panel 5B) as well as in individual myocytes (panel 5C–D). Comparison of the responses of individual myocytes within a field and the whole field response revealed that a uniform response could be maintained even though some individual myocytes did not respond uniformly at a given stimulation frequency (compare Figure 5B and 5C). Comparison of the whole field response for cultures transfected with wild type (WT) PITX2c and controls (pcDNA) showed that the intrinsic beating rate without electrical simulation and the ability to maintain a uniform response when the stimulation frequency was increased was similar ($p = 0.22$; ANOVA). Analysis of unstimulated cultures revealed no significant differences among different mutants. Inspection of the whole field beat-to-beat response of the different PITX2 mutant constructs upon electrical stimulation (Figure 6) revealed that the fraction of uniform responses was similar for cultures transfected with MD5 and pcDNA ($p = 0.65$; ANOVA) while MD4 ($p < 0.001$), MD4+5 ($p = 0.01$) and DN ($p = 0.002$) mutants all reduced the fraction of myocytes that were able to maintain a uniform beat-to-beat response. Fitting the fraction of uniform responses versus the stimulation frequency, using the Hill equation, is shown in the right hand panels of Figure 6A and fits are superimposed in Figure 6B with indication of the frequency where 50% of the preparations had a uniform response. The slope factor for the fits was near -4 and did not vary significantly for the different constructs. Figure 6C compares this frequency for the different PITX2c constructs. Analysis of the whole field non-uniform beat-to-beat responses revealed that MD4, MD5, MD4+5 and DN all presented a strong increase in irregular beat-to-beat patterns that often contained spontaneous calcium waves (Figure 7A,B). Interestingly, all constructs except the MD5 mutation showed alternating beat-to-beat responses or blockade (Figure 7C,D) that were most prominent at intermediate stimulation frequencies (1.3–2 Hz), suggesting that the underlying mechanisms may be different for the MD4 and MD5 variants.
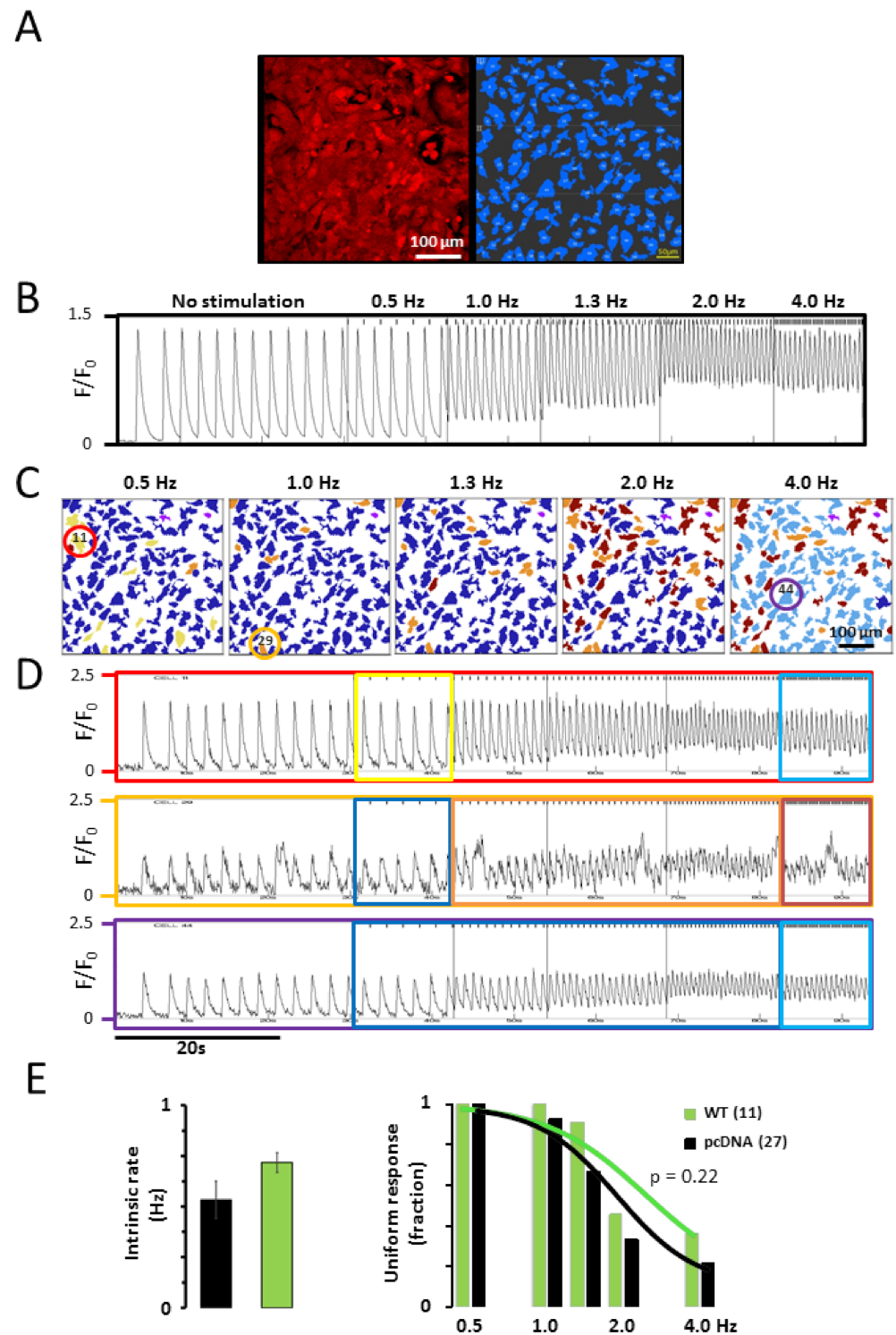
Figure 5. Calcium transient recordings in HL1 myocyte cultures. Panel (**A**). Calcium imaging in Cal-590 loaded HL1 myocytes (left) and automatic detection of myocytes with calcium signal (right). Panel (**B**). Calcium transient recorded in pcDNA transfected myocytes before (no stimulation) and after electrical field stimulation at the stimulation frequencies indicated above traces. Panel (**C**). Automatic classification of the calcium signals in individual HL1 myocytes. Color code indicates uniform (blue), alternating (yellow), block (light blue), waves (orange), or irregular (brown) beat-to-beat response. Panel (**D**). Responses of myocytes #11 (red), #29 (orange) and #44 (purple). Panel (**E**). The intrinsic beating rate (left) and the fraction of fields responding uniformly (right) were similar in cultures transfected with pcDNA and WT Pitx2. Number of experiments is given in parentheses.
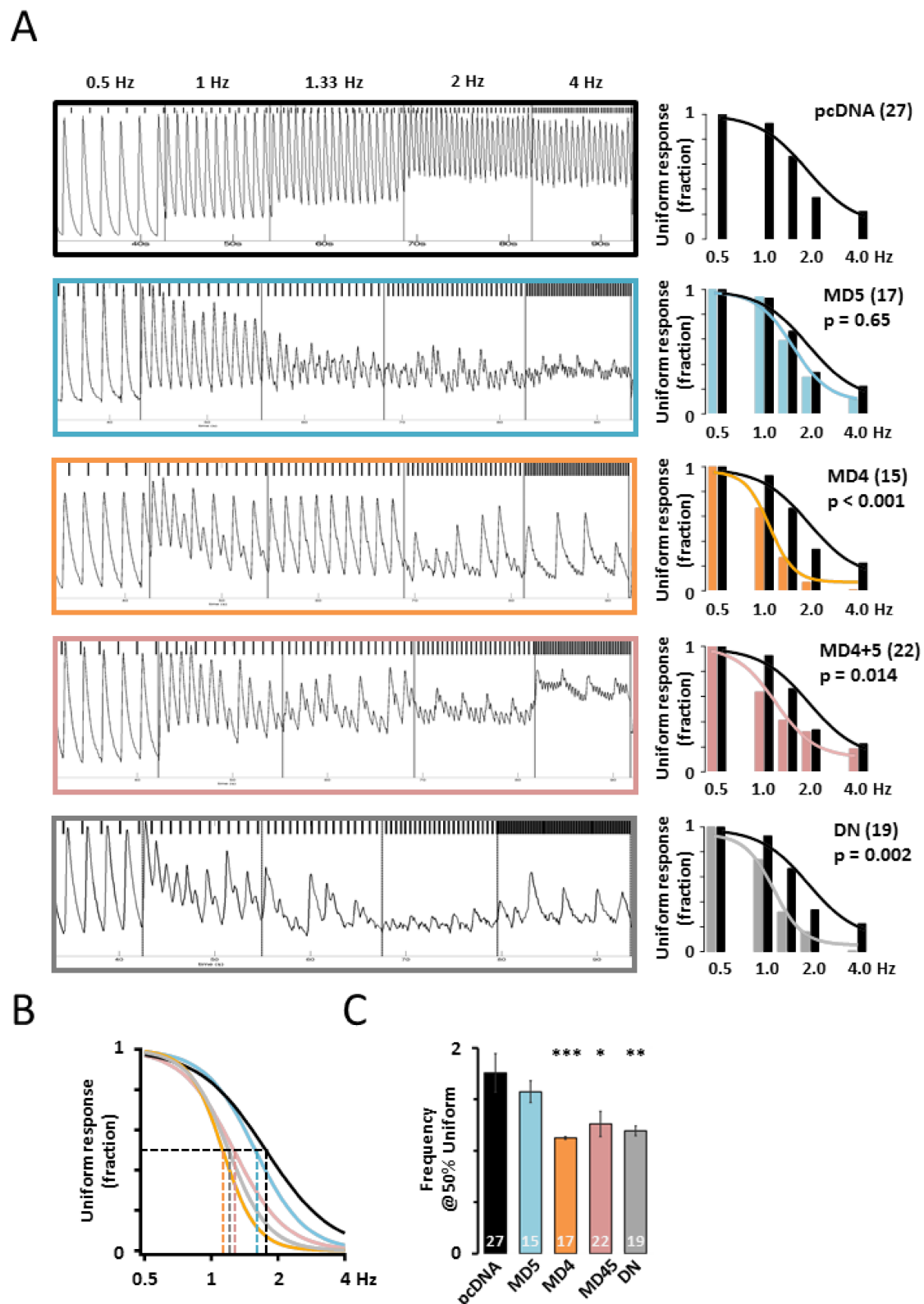
Figure 6. Impact of Pitx2 mutations on the beat-to-beat response. Panel (**A**). Traces of the beat-to-beat response recorded upon stepwise elevation of the stimulation frequency from 0.5 to 4 Hz are shown on the left for cultures transfected with pcDNA, DM5, DM4, DM4+5, or DN constructs. The corresponding fraction of uniform responses at the different stimulation frequencies is shown on the right and compared with pcDNA. Distributions of DM4, DM45 and DN were significantly different from the pcDNA distribution (ANOVA, *p*-values and n given for each construct). Data were fit with a Hill equation. Panel (**B**). Superimposed fits from panel (**C**) are shown on the left and the frequency where 50% responded uniformly is shown in (**C**). * *p* < 0.05, ** *p* < 0.01, *** *p* < 0.001.
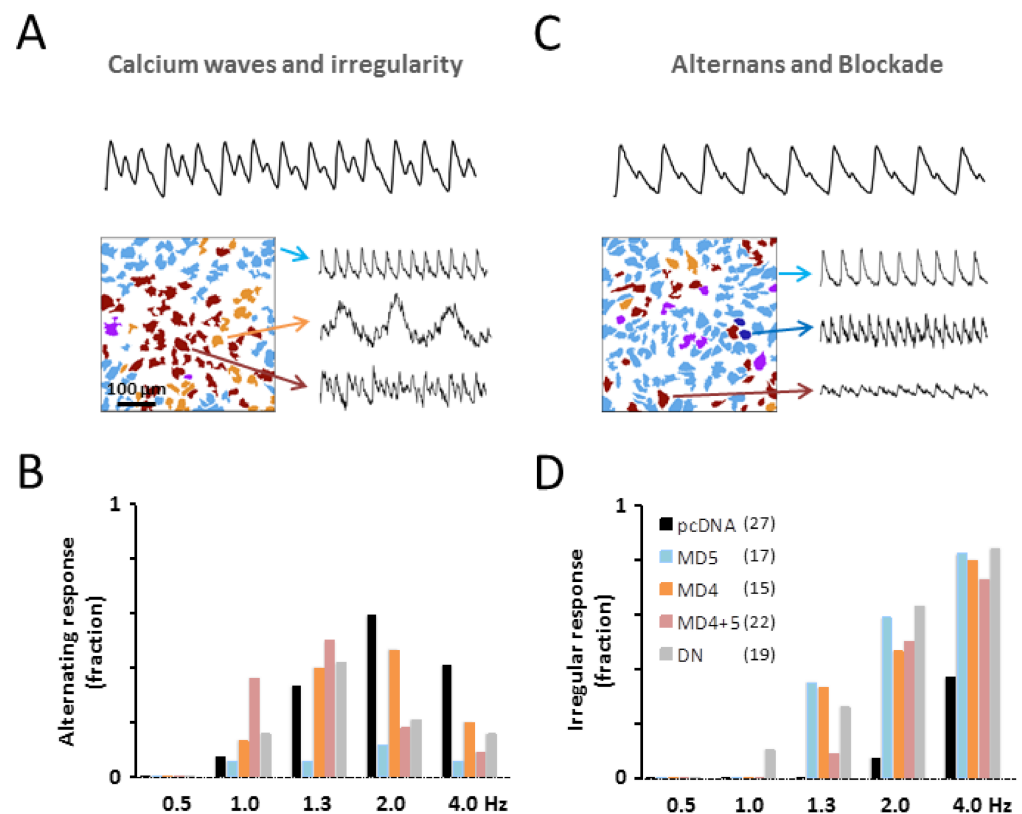
Figure 7. Pitx2 HD-mutants favor arrhythmic beat-to-beat responses. Panel (**A**). Traces of the beat-to-beat response in a whole image field presenting an irregular response. The response of individual myocytes in the field is shown below with traces from selected myocytes showing 1:1 block (light blue), waves (orange) and irregular responses (brown). Panel (**B**). Fraction of preparations transfected with pcDNA, MD5, MD4, MD4+5 or DN showing irregular responses at the stimulation frequency indicated below bars. Panel (**C**). Traces of the beat-to-beat response in a whole image field presenting an alternating response. The response of individual myocytes in the field is shown below with traces from selected myocytes showing 1:1 block (light blue), uniform (blue) and irregular responses (brown). Notice that the MD5 construct did barely induce alternating responses or block at any of the tested stimulation frequencies. Panel (**D**). Fraction of preparations transfected with pcDNA, MD5, MD4, MD4+5 or DN showing an irregular response at the stimulation frequency indicated below bars. When compared with pcDNA, all mutant Pitx2 construct increased the fraction of irregular responses ($p<0.01$, ANOVA). Number of experiments is given in parenthesis.

4. Discussion

Since atrial fibrillation was first associated with SNP risk variants at chromosome 4q25 that are located near PITX2 [2], research efforts have been undertaken to establish links between 4q25 risk variants and PITX2c activity [42,43], between PITX2c expression levels and AF [9,10,42,44] and to identify PITX2-mediated changes in the expression or activity of molecular mechanisms linked to AF [9,10,13]. Although it has been documented that the 4q25 variant rs2595104 reduces Pitx2 expression [43], the molecular events linking 4q25 risk variants, Pitx2 levels and AF still needs further clarification [42,44]. On the other hand, it has been documented that AF is associated with decreased Pitx2 expression [9] and that PITX2c loss of function predisposes to atrial arrhythmogenesis [9–12] and disturbances in the calcium homeostasis [13]. Moreover, the 4q25 risk variant rs13143308 has recently been linked to defective calcium homeostasis [14], pointing to *PITX2* as a candidate gene for AF associated with defective calcium homeostasis. The present study explores further the links between PITX2c function and AF, affording new evidence that mutations in the PITX2

HD identified in patients with AF, affects altogether PITX2c activity, calcium homeostasis and the beat-to-beat stability when expressed in HL1 cardiomyocyte cultures.

4.1. Impact of AF Associated PITX2 Homeodomain Mutants on PITX2c Function

Mutants identified in patients with AF and the MD4 and MD5 mutants caused amino acid substitutions are highly conserved region of the PITX2c homeodomain, increasing thus the likelihood that they might be detrimental. Indeed, both HD-variants were classified as potentially damaging. Interestingly, the patient carrying the MD4 and MD5 mutations had no 4q25 risk SNPs at rs2200733, rs13143308 or rs10033464, suggesting that the observed loss of PITX2 function is unrelated to 4q25 risk SNPs, which have previously been proposed to modify Pitx2 function [2,43]. Furthermore our data demonstrate that both novel PITX2 mutations alter the transactivation properties of PITX2c, both alone and in combination with cardiac-enriched transcription factors, such as Nkx2.5 and/or Gata4. Curiously, PITX2c transactivation impairment is rather similar between distinct mutations (MD4, MD5) when acting as a transcriptional activator (Nppa promoter), whereas some differences occur when PITX2c acts as a transcriptional repressor (Shox2 promoter). Furthermore, our data also demonstrate that no synergistic effects are observed by the presence of both mutations (MD4+5).

4.2. Impact of the PITX2 Mutants on Intracellular Calcium Homeostasis

The impact of loss of PITX2c function on ion channel expression and calcium homeostasis has previously been addressed in a mouse model of conditional atrial-specific PITX2c deletion [9,13]. Interestingly, we here found that the MD5, MD4+5 and DN mutants all reduced that SR calcium content while the content was similar for WT, pcDNA and the MD4 mutant. This observation is opposite to the mouse model where the SR calcium content was twice as high in left atrial myocytes from Pitx2$^{-/-}$ than from WT mice [13]. Similarly, Serca2, Pln and Casq mRNA levels were all increased in both left and right atria from Pitx2$^{-/-}$ mice [13] while we here observe a parallel reduction in Serca2 and Pln levels in MD4, MD5 and MD4+5 mutants as well as a reduced Casq level in the MD4+5 mutant. Nevertheless, the observed changes in SR calcium content are consistent with the observed differences in the calcium transient amplitude, which is reduced in the MD5 but not the MD4 variant. On the other hand, previous studies have associated paroxysmal AF [45] loss of PITX2c function [13] or 4q25 risk variants [14] with increased Serca2 expression and SR calcium content as well as a higher incidence of calcium waves, suggesting that another mechanism might be linking the PITX2 mutations to AF. In this regard, ventricular and atrial arrhythmia have also been associated with irregularities in the beat-to-beat response such as action potential and calcium transient alternans [46–49].

4.3. Impact of the PITX2 Mutants on the Rate-Dependency of the Beat-To-Beat Response

To test the latter hypothesis, we determined how the PITX2 mutations affected the beat-to-beat response of the calcium transient when cardiomyocyte cultures were subjected to increasing stimulation frequencies. Interestingly, only the MD4, MD4+5 and DN constructs induced a significant reduction in the fraction of uniform responses between 0.5 and 4 Hz, lowering the frequency where the fraction of uniform responses was reduced to 50%. Further analysis of the non-uniform beat-to-beat responses revealed that all PITX2c mutants significantly increased the incidence of irregular beat-to-beat responses while the MD5 mutation repressed alternating responses or blockade observed for the other PITX2c constructs as well as for cultures transfected with pcDNA. Considering that all mutants induce loss of PITX2c function (Figure 2A,B) while only the MD5 completely impairs PITX2c-dependent repression of Shox-2, it is conceivable that PITX2c insufficiency underlies the observed increase in irregular beat-to-beat responses in all PITX2c mutants. On the other hand, the absence of alternating responses in MD5 mutants might be related to the inability of this variant to repress Shox-2 activity. Because both MD4 and MD5 variants are associated with AF, these finding either suggests that the promotion of irregular beat-to-

beat responses is the key mechanisms contributing to the development of AF in the carrier of the MD4 and MD5 mutations. In support of this notion, human atrial myocytes from patients with AF have previously been shown to present a higher incidence of irregular beat-to-beat responses than myocytes from patients without AF [41]. Alternatively, several mechanisms may be acting in parallel to promote AF in the carrier of these mutations. In this regard, alternating responses have previously been linked to a high incidence of spontaneous calcium release events in human atrial myocytes [50], and RyR2 loss of function mutations causing severe ventricular arrhythmia have recently been linked to RyR2 inactivation and premature induction of calcium alternans [46,47].

In conclusion, we have identified two point mutations in the homeodomain of *PITX2* and three polymorphisms in the 5′untranslated region. Moreover, we document that the PITX2 HD point mutations cause loss of PITX2c function, impair Shox2 promoter repression as well as co-transactivation with other cardiac-enriched co-factors such as Gata4 and Nkx2.5, pointing to a pivotal role for these mutations for correct PITX2c function. The mutations also impaired endogenous expression of calcium regulatory proteins and alterations in sarcoplasmic reticulum (SR) calcium accumulation that favored alternating and irregular calcium transient amplitudes, causing deterioration of the beat-to-beat stability upon elevation of the stimulation frequency. Together, this data demonstrate that these novel PITX2 mutations may contribute to the development of atrial fibrillation in the patient carrying them.

Author Contributions: Conceptualization, E.D., R.C., A.A., D.F. and L.H.-M.; Formal analysis, A.H.-M., C.T., E.L.-V., V.J.-S., S.C., F.H.-T., H.D., E.V.R.d.C., A.A., D.F. and L.H.-M.; Funding acquisition, D.F. and L.H.-M.; Investigation, A.H.-M., C.T., E.L.-V., V.J.-S., S.C., F.H.-T., H.D., E.V.R.d.C., E.D., R.C. and A.A.; Methodology, A.H.-M., C.T., E.L.-V., V.J.-S., S.C., F.H.-T., H.D., E.V.R.d.C., E.D., R.C. and A.A.; Supervision, D.F. and L.H.-M.; Writing—original draft, D.F. and L.H.-M. All authors have read and agreed to the published version of the manuscript.

Institutional Review Board Statement: The study was conducted according to the guidelines of the Declaration of Helsinki, and approved by the Ethics Committee at Hospital Regional de Jaén.

Informed Consent Statement: Informed consent was obtained from all subjects involved in the study.

Data Availability Statement: Not applicable.

Conflicts of Interest: The authors declare no conflict of interest.

References

1. Camm, A.J.; Lip, G.Y.; De Caterina, R.; Savelieva, I.; Atar, D.; Hohnloser, S.H.; Hindricks, G.; Kirchhof, P.; Bax, J.J.; Baumgartner, H.; et al. 2012 focused update of the ESC Guidelines for the management of atrial fibrillation. *Eur. Hear. J.* **2012**, *33*, 2719–2747. [CrossRef]
2. Gudbjartsson, D.F.; Arnar, D.O.; Helgadottir, A.; Gretarsdottir, S.; Holm, H.; Sigurdsson, A.; Jonasdottir, A.; Baker, A.; Thorleifsson, G.; Kristjansson, K.; et al. Variants conferring risk of atrial fibrillation on chromosome 4q25. *Nat. Cell Biol.* **2007**, *448*, 353–357. [CrossRef] [PubMed]
3. Lubitz, S.A.; Sinner, M.F.; Lunetta, K.L.; Makino, S.; Pfeufer, A.; Rahman, R.; Veltman, C.E.; Barnard, J.; Bis, J.C.; Danik, S.P.; et al. Independent Susceptibility Markers for Atrial Fibrillation on Chromosome 4q25. *Circulation* **2010**, *122*, 976–984. [CrossRef]
4. Lubitz, S.A.; Lunetta, K.L.; Lin, H.; Arking, D.E.; Trompet, S.; Li, G.; Krijthe, B.P.; Chasman, D.I.; Barnard, J.; Kleber, M.E.; et al. Novel Genetic Markers Associate With Atrial Fibrillation Risk in Europeans and Japanese. *J. Am. Coll. Cardiol.* **2014**, *63*, 1200–1210. [CrossRef] [PubMed]

5. Nielsen, J.B.; Thorolfsdottir, R.B.; Fritsche, L.G.; Zhou, W.; Skov, M.W.; Graham, S.E.; Herron, T.J.; McCarthy, S.; Schmidt, E.M.; Sveinbjornsson, G.; et al. Biobank-driven genomic discovery yields new insight into atrial fibrillation biology. *Nat. Genet.* **2018**, *50*, 1234–1239. [CrossRef]

6. Franco, D. The Role of Pitx2 during Cardiac Development Linking Left–Right Signaling and Congenital Heart Diseases. *Trends Cardiovasc. Med.* **2003**, *13*, 157–163. [CrossRef]

7. Campione, M.; Ros, M.A.; Icardo, J.M.; Piedra, E.; Christoffels, V.M.; Schweickert, A.; Blum, M.; Franco, D.; Moorman, A.F. Pitx2 Expression Defines a Left Cardiac Lineage of Cells: Evidence for Atrial and Ventricular Molecular Isomerism in the iv/iv Mice. *Dev. Biol.* **2001**, *231*, 252–264. [CrossRef]

8. Mommersteeg, M.T.M.; Brown, N.A.; Prall, O.W.J.; Vries, C.D.G.-D.; Harvey, R.P.; Moorman, A.F.M.; Christoffels, V.M. Pitx2c and Nkx2-5 Are Required for the Formation and Identity of the Pulmonary Myocardium. *Circ. Res.* **2007**, *101*, 902–909. [CrossRef]

9. Chinchilla, A.; Daimi, H.; Lozano-Velasco, E.; Dominguez, J.N.; Caballero, R.; Delpón, E.; Tamargo, J.; Cinca, J.; Hove-Madsen, L.; Aranega, A.E.; et al. PITX2 Insufficiency Leads to Atrial Electrical and Structural Remodeling Linked to Arrhythmogenesis. *Circ. Cardiovasc. Genet.* **2011**, *4*, 269–279. [CrossRef]

10. Kirchhof, P.; Kahr, P.C.; Kaese, S.; Piccini, I.; Vokshi, I.; Scheld, H.-H.; Rotering, H.; Fortmueller, L.; Laakmann, S.; Verheule, S.; et al. PITX2c Is Expressed in the Adult Left Atrium, and Reducing Pitx2c Expression Promotes Atrial Fibrillation Inducibility and Complex Changes in Gene Expression. *Circ. Cardiovasc. Genet.* **2011**, *4*, 123–133. [CrossRef]

11. Wang, J.; Klysik, E.; Sood, S.; Johnson, R.L.; Wehrens, X.H.T.; Martin, J.F. Pitx2 prevents susceptibility to atrial arrhythmias by inhibiting left-sided pacemaker specification. *Proc. Natl. Acad. Sci. USA* **2010**, *107*, 9753–9758. [CrossRef] [PubMed]

12. Collins, M.M.; Ahlberg, G.; Hansen, C.V.; Guenther, S.; Marín-Juez, R.; Sokol, A.M.; El-Sammak, H.; Piesker, J.; Hellsten, Y.; Olesen, M.S.; et al. Early sarcomere and metabolic defects in a zebrafish pitx2c cardiac arrhythmia model. *Proc. Natl. Acad. Sci. USA* **2019**, *116*, 24115–24121. [CrossRef] [PubMed]

13. Lozano-Velasco, E.; Hernández-Torres, F.; Daimi, H.; Serra, S.A.; Herraiz, A.; Hove-Madsen, L.; Aránega, A.; Franco, D. Pitx2 impairs calcium handling in a dose-dependent manner by modulating Wnt signalling. *Cardiovasc. Res.* **2016**, *109*, 55–66. [CrossRef] [PubMed]

14. Herraiz-Martínez, A.; Llach, A.; Tarifa, C.; Gandía, J.; Jiménez-Sabado, V.; Lozano-Velasco, E.; Serra, S.A.; Vallmitjana, A.; De Castroviejo, E.V.R.; Benítez, R.; et al. The 4q25 variant rs13143308T links risk of atrial fibrillation to defective calcium homoeostasis. *Cardiovasc. Res.* **2019**, *115*, 578–589. [CrossRef]

15. Semina, E.V.; Reiter, R.; Leysens, N.J.; Alward, W.L.M.; Small, K.W.; Datson, N.A.; Siegel-Bartelt, J.; Bierke-Nelson, D.; Bitoun, P.; Zabel, B.U.; et al. Cloning and characterization of a novel bicoid-related homeobox transcription factor gene, RIEG, involved in Rieger syndrome. *Nat. Genet.* **1996**, *14*, 392–399. [CrossRef]

16. Priston, M.; Kozlowski, K.; Gill, D.; Letwin, K.; Buys, Y.; Levin, A.V.; Walter, M.A.; Héon, E. Functional analyses of two newly identified PITX2 mutants reveal a novel molecular mechanism for Axenfeld-Rieger syndrome. *Hum. Mol. Genet.* **2001**, *10*, 1631–1638. [CrossRef]

17. Reis, L.M.; Tyler, R.C.; Kloss, B.A.V.; Schilter, K.F.; Levin, A.V.; Lowry, R.B.; Zwijnenburg, P.J.G.; Stroh, E.; Broeckel, U.; Murray, J.C.; et al. PITX2 and FOXC1 spectrum of mutations in ocular syndromes. *Eur. J. Hum. Genet.* **2012**, *20*, 1224–1233. [CrossRef]

18. Yun, J.W.; Cho, H.-K.; Oh, S.-Y.; Ki, C.-S.; Kee, C. Novel c.300_301delinsT Mutation in PITX2 in a Korean Family with Axenfeld-Rieger Syndrome. *Ann. Lab. Med.* **2013**, *33*, 360–363. [CrossRef]

19. Yin, H.-F.; Fang, X.-Y.; Jin, C.-F.; Yin, J.-F.; Li, J.-Y.; Zhao, S.-J.; Miao, Q.; Song, F.-W. Identification of a novel frameshift mutation in PITX2 gene in a Chinese family with Axenfeld-Rieger syndrome. *J. Zhejiang Univ. Sci. B* **2014**, *15*, 43–50. [CrossRef]

20. Alward, W.L.; Semina, E.V.; Kalenak, J.W.; Héon, E.; Sheth, B.P.; Stone, E.M.; Murray, J.C. Autosomal dominant iris hypoplasia is caused by a mutation in the Rieger syndrome (RIEG/PITX2) gene. *Am. J. Ophthalmol.* **1998**, *125*, 98–100. [CrossRef]

21. Doward, W.; Perveen, R.; Lloyd, I.C.; Ridgway, A.; Wilson, L.; Black, G.C. A mutation in the RIEG1 gene associated with Peters' anomaly. *J. Med. Genet.* **1999**, *36*, 152–155.

22. Xia, K. Mutation in PITX2 is associated with ring dermoid of the cornea. *J. Med. Genet.* **2004**, *41*, e129. [CrossRef] [PubMed]

23. Wang, J.; Xin, Y.-F.; Xu, W.-J.; Liu, Z.-M.; Qiu, X.-B.; Qu, X.-K.; Xu, L.; Li, X.; Yang, Y.-Q. Prevalence and Spectrum of PITX2c Mutations Associated with Congenital Heart Disease. *DNA Cell Biol.* **2013**, *32*, 708–716. [CrossRef] [PubMed]

24. Martin, D.M.; Probst, F.J.; Fox, S.E.; Schimmenti, L.A.; Semina, E.V.; Hefner, M.A.; Belmont, J.W.; Camper, S.A. Exclusion ofPITX2 mutations as a major cause of CHARGE association. *Am. J. Med. Genet.* **2002**, *111*, 27–30. [CrossRef] [PubMed]

25. Mechakra, A.; Footz, T.; Walter, M.; Aránega, A.; Hernández-Torres, F.; Morel, E.; Millat, G.; Yang, Y.-Q.; Chahine, M.; Chevalier, P.; et al. A Novel PITX2c Gain-of-Function Mutation, p.Met207Val, in Patients With Familial Atrial Fibrillation. *Am. J. Cardiol.* **2019**, *123*, 787–793. [CrossRef] [PubMed]

26. Mora, C.; Serzanti, M.; Giacomelli, A.; Beltramone, S.; Marchina, E.; Bertini, V.; Piovani, G.; Refsgaard, L.; Olesen, M.S.; Cortellini, V.; et al. Generation of induced pluripotent stem cells (iPSC) from an atrial fibrillation patient carrying a PITX2 p.M200V mutation. *Stem. Cell Res.* **2017**, *24*, 8–11. [CrossRef]

27. Tsai, C.-T.; Hsieh, C.-S.; Chang, S.-N.; Chuang, E.Y.; Juang, J.-M.J.; Lin, L.-Y.; Lai, L.-P.; Hwang, J.-J.; Chiang, F.-T.; Lin, J.-L. Next-generation sequencing of nine atrial fibrillation candidate genes identified novel de novo mutations in patients with extreme trait of atrial fibrillation. *J. Med. Genet.* **2015**, *52*, 28–36. [CrossRef]

28. Zhou, Y.; Zheng, P.; Yang, Y.; Ge, Z.; Kang, W. A novel PITX2c loss-of-function mutation underlies lone atrial fibrillation. *Int. J. Mol. Med.* **2013**, *32*, 827–834. [CrossRef]

29. Boldt, L.-H.; Posch, M.G.; Perrot, A.; Polotzki, M.; Rolf, S.; Parwani, A.S.; Huemer, M.; Wutzler, A.; Özcelik, C.; Haverkamp, W. Mutational analysis of the PITX2 and NKX2-5 genes in patients with idiopathic atrial fibrillation. *Int. J. Cardiol.* **2010**, *145*, 316–317. [CrossRef]

30. Yang, Y.-Q.; Xu, Y.-J.; Li, R.-G.; Qu, X.-K.; Fang, W.-Y.; Liu, X. Prevalence and spectrum of PITX2c mutations associated with familial atrial fibrillation. *Int. J. Cardiol.* **2013**, *168*, 2873–2876. [CrossRef]

31. Wang, J.; Zhang, D.-F.; Sun, Y.-M.; Yang, Y.-Q. A novel PITX2c loss-of-function mutation associated with familial atrial fibrillation. *Eur. J. Med. Genet.* **2014**, *57*, 25–31. [CrossRef]

32. Toro, R.; Saadi, I.; Kuburas, A.; Nemer, M.; Russo, A.F. Cell-specific Activation of the Atrial Natriuretic Factor Promoter by PITX2 and MEF2A. *J. Biol. Chem.* **2004**, *279*, 52087–52094. [CrossRef]

33. Ganga, M.; Espinoza, H.M.; Cox, C.J.; Morton, L.; Hjalt, T.A.; Lee, Y.; Amendt, B.A. PITX2 Isoform-specific Regulation of Atrial Natriuretic Factor Expression. *J. Biol. Chem.* **2003**, *278*, 22437–22445. [CrossRef] [PubMed]

34. Dunnen, J.T.D.; Antonarakis, S.E. Nomenclature for the description of human sequence variations. *Hum. Genet.* **2001**, *109*, 121–124. [CrossRef] [PubMed]

35. Knowlton, K.U.; Baracchini, E.; Ross, R.S.; Harris, A.N.; Henderson, S.A.; Evans, S.M.; Glembotski, C.C.; Chien, K.R. Co-regulation of the atrial natriuretic factor and cardiac myosin light chain-2 genes during alpha-adrenergic stimulation of neonatal rat ventricular cells. Identification of cis sequences within an embryonic and a constitutive contractile protein gene which mediate inducible expression. *J Biol Chem.* **1991**, *266*, 7759–7768. [CrossRef] [PubMed]

36. Lee, Y.; Shioi, T.; Kasahara, H.; Jobe, S.M.; Wiese, R.J.; Markham, B.E.; Izumo, S. The cardiac tissue-restricted homeobox protein Csx/Nkx2.5 physically associates with the zinc finger protein GATA4 and cooperatively activates atrial natriuretic factor gene expression. *Mol. Cell Biol.* **1998**, *18*, 3120–3129. [CrossRef]

37. Hernández-Torres, F.; Rastrojo, A.; Aguado, B. Intron retention and transcript chimerism conserved across mammals: Ly6g5b and Csnk2b-Ly6g5b as examples. *BMC Genom.* **2013**, *14*, 199. [CrossRef]

38. Hernández-Torres, F.; Aránega, A.E.; Franco, D. Identification of regulatory elements directing miR-23a–miR-27a–miR-24-2 transcriptional regulation in response to muscle hypertrophic stimuli. *Biochim. Biophys. Acta (BBA) Bioenerg.* **2014**, *1839*, 885–897. [CrossRef]

39. Bustin, S.A.; Benes, V.; Garson, J.A.; Hellemans, J.; Huggett, J.; Kubista, M.; Mueller, R.; Nolan, T.; Pfaffl, M.W.; Shipley, G.L.; et al. The MIQE Guidelines: Minimum Information for Publication of Quantitative Real-Time PCR Experiments. *Clin. Chem.* **2009**, *55*, 611–622. [CrossRef]

40. Livak, K.J.; Schmittgen, T.D. Analysis of Relative Gene Expression Data Using Real-Time Quantitative PCR and the $2^{-\Delta\Delta CT}$ Method. *Methods* **2001**, *25*, 402–408. [CrossRef]

41. Molina, C.E.; Llach, A.; Herraiz-Martínez, A.; Tarifa, C.; Barriga, M.; Wiegerinck, R.F.; Fernandes, J.; Cabello, N.; Vallmitjana, A.; Benitez, R.; et al. Prevention of adenosine A2A receptor activation diminishes beat-to-beat alternation in human atrial myocytes. *Basic Res. Cardiol.* **2015**, *111*, 1–15. [CrossRef]

42. Syeda, F.; Holmes, A.P.; Yu, T.Y.; Tull, S.; Kuhlmann, S.M.; Pavlovic, D.; Betney, D.; Riley, G.; Kucera, J.P.; Jousset, F.; et al. PITX2 Modulates Atrial Membrane Potential and the Antiarrhythmic Effects of Sodium-Channel Blockers. *J. Am. Coll. Cardiol.* **2016**, *68*, 1881–1894. [CrossRef] [PubMed]

43. Ye, J.; Tucker, N.R.; Weng, L.-C.; Clauss, S.; Lubitz, S.A.; Ellinor, P.T. A Functional Variant Associated with Atrial Fibrillation Regulates PITX2c Expression through TFAP2a. *Am. J. Hum. Genet.* **2016**, *99*, 1281–1291. [CrossRef]

44. Gore-Panter, S.R.; Hsu, J.; Hanna, P.; Gillinov, A.M.; Pettersson, G.; Newton, D.W.; Moravec, C.S.; Van Wagoner, D.R.; Chung, M.K.; Barnard, J.; et al. Atrial Fibrillation Associated Chromosome 4q25 Variants Are Not Associated with PITX2c Expression in Human Adult Left Atrial Appendages. *PLoS ONE* **2014**, *9*, e86245. [CrossRef] [PubMed]

45. Voigt, N.; Heijman, J.; Wang, Q.; Chiang, D.Y.; Li, N.; Karck, M.; Wehrens, X.H.; Nattel, S.; Dobrev, D. Cellular and Molecular Mechanisms of Atrial Arrhythmogenesis in Patients With Paroxysmal Atrial Fibrillation. *Circulation* **2014**, *129*, 145–156. [CrossRef] [PubMed]

46. Sun, B.; Yao, J.; Ni, M.; Wei, J.; Zhong, X.; Guo, W.; Zhang, L.; Wang, R.; Belke, D.; Chen, Y.-X.; et al. Cardiac ryanodine receptor calcium release deficiency syndrome. *Sci. Transl. Med.* **2021**, *13*, eaba7287. [CrossRef] [PubMed]

47. Wei, J.; Yao, J.; Belke, D.; Guo, W.; Zhong, X.; Sun, B.; Wang, R.; Estillore, J.P.; Vallmitjana, A.; Benitez, R.; et al. Ca 2+ -CaM Dependent Inactivation of RyR2 Underlies Ca 2+ Alternans in Intact Heart. *Circ. Res.* **2021**, *128*. [CrossRef] [PubMed]

48. Lalani, G.G.; Schricker, A.A.; Clopton, P.; Krummen, D.E.; Narayan, S.M. Frequency Analysis of Atrial Action Potential Alternans. *Circ. Arrhythmia Electrophysiol.* **2013**, *6*, 859–867. [CrossRef]

49. Liu, T.; Xiong, F.; Qi, X.-Y.; Xiao, J.; Villeneuve, L.; Abu-Taha, I.; Dobrev, D.; Huang, C.; Nattel, S. Altered calcium handling produces reentry-promoting action potential alternans in atrial fibrillation–remodeled hearts. *JCI Insight* **2020**, *5*. [CrossRef]

50. Llach, A.; Molina, C.E.; Fernandes, J.; Padro, J.; Cinca, J.; Hove-Madsen, L. Sarcoplasmic reticulum and L-type Ca2+channel activity regulate the beat-to-beat stability of calcium handling in human atrial myocytes. *J. Physiol.* **2011**, *589*, 3247–3262. [CrossRef]